

# Collapsible Underwater Docking Station Design and Evaluation\*

Brian R. Page<sup>1</sup>, John Naglak<sup>1</sup>, Caleb Kase<sup>2</sup>, and Nina Mahmoudian<sup>3</sup>

**Abstract**— Persistent undersea operation is dependent on effective and accessible underwater docking and charging mechanisms for autonomous underwater vehicles (AUVs). Existing docking stations are able to support extended operations with one specific AUV and generally require extensive modification to the AUV to function. This paper presents a new underwater docking station that can support a wide range of AUVs with minimal modification required. Key aspects of the docking station design are the simplified funnel design that reduces manufacturing and deployment complexity and the docking adapter. The adapter can be used as a drop-in replacement for a more traditional AUV antenna with the addition of recharging electronics. It is the only component that contacts the docking station meaning that one station can support AUVs over a wide range of designs and sizes. This work is focused on optimization of the terminal homing stage for docking. Specifically, the effect of impact velocity relative to capture envelope and impact force is studied. Based on the initial optimization of the docking system, a target impact velocity of 1.0m/s results in the largest effective capture envelope and the minimum impact force when using a Dolphin II AUV.

**Index Terms**— Marine Robotics; Optimization and Optimal Control; Mechanism Design; Docking; Dynamics

## I. INTRODUCTION

Exploration of the ocean with autonomous underwater vehicles (AUVs) has increased over the past decade as vehicle costs have come down while sensor quality and endurance have improved. However, AUVs are still very expensive to operate on multi-day missions away from shore due to the manned surface vessel required to support recharging. One solution to the endurance limitation of AUVs is automated docking and recharging [1]. Several autonomous docking stations have been developed that support recharging of AUVs independent of a manned vessel [2], [3].

Existing docking stations are typically of the funnel [4], [5] or pole [6] design. Funnel based designs feature the largest capture envelopes and have seen the widest adoption. The effective capture envelope is the most critical design element of any docking station as it defines the success or failure of the system once it is deployed. Secondary factors

\*This material is based upon work supported by the National Science Foundation under grant no 1453886 and Office of Naval Research N00014-15-1-2599.

<sup>1</sup>Brian R. Page and John Naglak are Graduate Research Assistants with the Department of Mechanical Engineering-Engineering Mechanics, Michigan Technological University, Houghton, MI, USA bpage@mtu.edu, jenaglak@mtu.edu

<sup>2</sup>Caleb Kase is an Undergraduate Research Assistant with the Department of Mechanical Engineering-Engineering Mechanics, Michigan Technological University, Houghton, MI, USA cdkase@mtu.edu

<sup>3</sup>Nina Mahmoudian is the Lou and Herbert Wacker Associate Professor in Autonomous Mobile Systems with the Department of Mechanical Engineering-Engineering Mechanics, Michigan Technological University, Houghton, MI, USA ninam@mtu.edu

in docking station adoption are the cost of the system and the adaptability to other AUVs. The adaptability to multiple AUVs is one of the main limiting factors in deployments of docking stations. Existing docking stations are either specific to one AUV like the funnel based designs [4], [5], or require modification to critical areas of the AUV like the pole based designs [6]. The ability to support a wide variety of AUVs (including different size classes) without requiring significant modification has not existed prior to this work.

Control and navigation of an AUV during docking is typically broken into five stages: en route, approach setup, approach, terminal homing, and capture [2]. The en route step involves navigating the AUV using long range navigation such as dead-reckoning to come within range of the docking sensors. Once within range of near navigation sensors, the vehicle sets itself up for the approach phase by reaching a point directly in line with the dock. The approach is typically a direct approach, although more advanced methods do exist such as the hybrid sliding approach [7] and a fuzzy approach [8]. Terminal homing is the final few meters before docking and is used to improve accuracy with high accuracy feedback. The capture stage is the final stage during the impact with the docking station where the vehicle continues to thrust until latched. This work focuses on the terminal homing and capture stages as the other stages are the same regardless of docking station design.

We are proposing a new docking system that aims to reduce the cost of deployment and increase the flexibility of docking stations. The adaptive docking system is a lightweight docking station and docking adapter that features a relatively large capture envelope, is easy to deploy, and can support a range of AUVs. Key to the docking systems functionality is the unique docking adapter design that is meant as a drop-in replacement for an AUVs antenna mast. The docking adapter is the only component that requires customization to the AUV. This design idea enables nearly any AUV to dock with one standardized docking station allowing the docking station to serve as a recharging point for any AUV in the area. This paper presents the optimization of impact velocity for the docking station using a co-simulation based approach. Optimal choice of impact velocity can maximize the effective capture envelope while minimizing the peak impact force, both critical aspects of any docking station. The characteristics of the terminal homing stage will be dependent on the size of AUV used.

The remainder of this paper presents the detailed docking system in Sec. II, the dynamic model and simulation in Sec. III, results in Sec. IV, and a brief conclusion in Sec. V.

## II. DOCKING SYSTEM DESIGN

The adaptive docking system is able to support docking of a wide variety of AUVs with a single fixed docking station. This is due to the unique capture design consisting of the fixed docking station and the docking adapter. The fixed docking station is of a simplified cone design, reducing it from a fully three dimensional cone into a simplified funnel design with a ramp. The simplified funnel allows a large capture envelope in the horizontal plane while the ramp enables a sufficient vertical plane capture envelope. The unique simplified funnel design enables reduced manufacturing and deployment costs compared to traditional cone designs. Further, the simplified funnel enables docking stations to be collapsed for storage and transport.

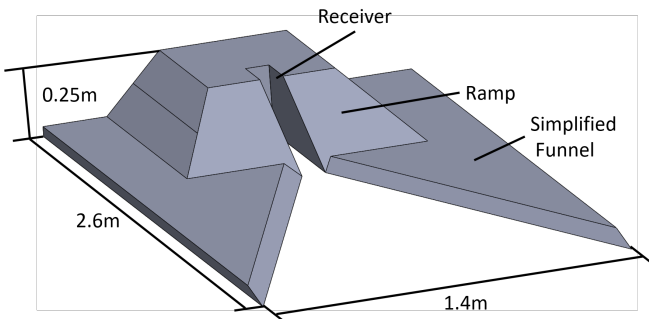


Fig. 1: The docking station consists of the receiver, simplified funnel, ramp, non-contact latch (not shown), and recharging transmission systems (not shown). The docking station enables the large capture area inherent in a cone shaped design while still being capable of supporting a wide range of AUVs.

The docking station (Fig. 1) design consists of the receiver, simplified funnel, ramp, non-contact latch, and power/data transmission systems. The receiver, simplified funnel, and ramp are fixed frame pieces that serve to hold the AUV during charging, guide the AUV along the horizontal plane, and guide the AUV along the vertical plane respectively. The non-contact latching system consists of an electropermanent magnet mounted on the underside of the docking station. The electropermanent magnet couples with a corresponding ferrous piece on the docking adapter. The power/data transmission system is an inductive power module. The inductive system is rated to 50W through seawater and also generates a short range WiFi network for data transmission between AUV and docking station. Following validation, the inductive system can be scaled up to 3kW for rapid recharging of the AUV. With a 3kW rate, AUVs could be recharged at a similar rate to shipboard recharging. Once battery technology supports it, vehicles such as the Iver 3 could be recharged in 20 minutes.

The docking adapter (Fig. 2) is a one piece design that mounts on top of any traditional AUV and is meant to serve as a drop-in replacement for the standard antenna mast. The adapter features the mast, guide planes, power/data transmission electronics, and non-contact latching system. The mast

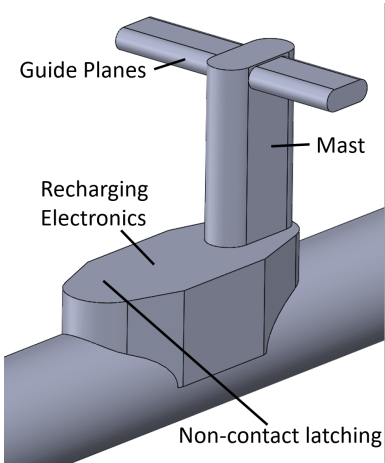


Fig. 2: The docking adapter sits on top of the AUV as a drop-in replacement for an external antenna mast. The adapter consists of a mast, guide planes, recharging electronics, and the non-contact latching system.

serves to guide the AUV along the docking station simplified funnel in the horizontal plane and can be customized to contain the antennas required for the specific AUV. The guide planes function to raise the AUV into the docking station receiver by sliding up the ramp. The recharging electronics are the receiving end of the inductive power module. This system contains the power conditioning required to support recharging of the AUV onboard battery pack. Finally, the non-contact latching system is a piece of ferrous material forward of the recharging electronics that clamps to the electropermanent magnet located on the docking station.

During operation, the docking station will be installed either on the seafloor or on any marine system that is large enough such that a fully fixed assumption can apply during docking. The docking procedure is as follows:

- 1) The AUV approaches the docking station using long distance navigation.
- 2) Once within range of the docking station homing system it enters into a docking controller.
- 3) The docking controller drives the AUV toward the docking station trying to maintain cross track error to zero.
- 4) The docking adapter mounted atop the AUV impacts the docking station and begins guiding the AUV into the station.
- 5) The docking adapter slides along the station funnel and then slides up the station ramp though the use of the guide planes.
- 6) Once inside the docking station the non-contact latching system is enabled to securely fasten the AUV inside the docking station for charging.
- 7) Power and data are transferred wirelessly through the inductive power module.
- 8) Following charging, the AUV undocks by disabling the non-contact latching system and reverses to a safe distance before resuming its mission.

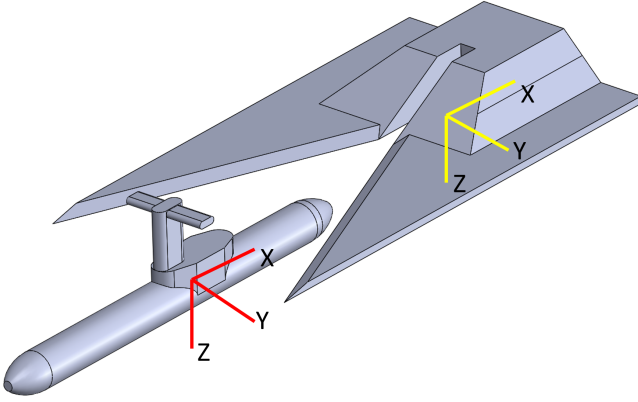


Fig. 3: The body-fixed frame (red) is located on the AUV. The earth-fixed frame (yellow) is located on the docking station. Docking is successful when the two frames overlap.

As with any underwater docking system, failed dockings are expected due to the difficulties of accurate localization and actuation in the subsea environment. In the event of a failed docking attempt the AUV will recognize the failure, navigate to the start of the docking profile, and restart the docking procedure.

### III. DYNAMIC MODELLING & SIMULATION

The dynamic model presented here is built on work in [9], [10], and is general to traditional AUVs with vehicle specific coefficients available in [9].

Several key assumptions are required to simplify the dynamic model such that it can be efficiently solved.

- 1) Docking occurs in deep, calm water such that disturbances can be ignored.
- 2) The AUV is neutrally buoyant in the water with a small self-righting moment due to the distance between center of mass and center of buoyancy.
- 3) The docking station is fully fixed.
- 4) No significant deformation occurs to either the AUV or docking station during docking.
- 5) Impact can be effectively modelled as a spring-damper.
- 6) The thruster is a constant forward force.

Two coordinate frames are used to model the docking process, the body-fixed frame located on the AUV and earth-fixed frame located in the docking station. Both frames follow SNAME orientation (north-east-down) [11] (Fig. 3). Docking is considered successful when the two frames overlap.

The vehicle hydrodynamic model can be broken into viscous and inviscid terms, which can then be added back together due to superposition. The viscous terms include both

forces ( $f_v$ ) and moments ( $m_v$ ) as follows:

$$\begin{aligned} \mathbf{f}_v &= \begin{pmatrix} X_v \\ Y_v \\ Z_v \end{pmatrix} \\ \mathbf{m}_v &= \begin{pmatrix} K_v \\ M_v \\ N_v \end{pmatrix} \end{aligned} \quad (1)$$

The forces and moments can be non-dimensionalized and then calculated following Eqn. 2 and 3 [12], [13].

$$\begin{aligned} X'_v &= \frac{X_v}{0.5\rho V^2 L^2}, & Y'_v &= \frac{Y_v}{0.5\rho V^2 L^2}, & Z'_v &= \frac{Z_v}{0.5\rho V^2 L^2} \\ K'_v &= \frac{K_v}{0.5\rho V^2 L^3}, & M'_v &= \frac{M_v}{0.5\rho V^2 L^3}, & N'_v &= \frac{N_v}{0.5\rho V^2 L^3} \end{aligned} \quad (2)$$

$$\begin{aligned} X'_v &= C_X(\alpha) = C_X^0 + C_X^{\alpha_1}\alpha + C_X^{\alpha_2}\alpha^2 + C_X^{\alpha_3}\alpha^3 + C_X^{\alpha_4}\alpha^4 \\ K'_v &= C_K(\beta, \bar{p}, \bar{r}, \delta_r) = C_K^{\beta}\beta + C_K^{\bar{p}}\bar{p} + C_K^{\bar{r}}\bar{r} + C_K^{\delta_r}\delta_r \\ Y'_v &= C_Y(\beta, \bar{p}, \bar{r}, \delta_r) = C_Y^{\beta}\beta + C_Y^{\bar{p}}\bar{p} + C_Y^{\bar{r}}\bar{r} + C_Y^{\delta_r}\delta_r \\ M'_v &= C_M(\alpha, \bar{q}, \delta_e) = C_M^{\alpha}\alpha + C_M^{\bar{q}}\bar{q} + C_M^{\delta_e}\delta_e \\ Z'_v &= C_Z(\alpha, \bar{q}, \delta_e) = C_Z^{\alpha}\alpha + C_Z^{\bar{q}}\bar{q} + C_Z^{\delta_e}\delta_e \\ N'_v &= C_N(\beta, \bar{p}, \bar{r}, \delta_r) = C_N^{\beta}\beta + C_N^{\bar{p}}\bar{p} + C_N^{\bar{r}}\bar{r} + C_N^{\delta_r}\delta_r \end{aligned} \quad (3)$$

Where  $V$  is total vehicle velocity,  $L$  is characteristic length,  $\alpha$  is angle of attack,  $\beta$  is sideslip angle,  $\delta_r$  and  $\delta_e$  are rudder and elevator angles. The AUV angular velocities are non-dimensionalized following  $\bar{p} = \frac{pL}{V}$ ,  $\bar{q} = \frac{qL}{V}$ , and  $\bar{r} = \frac{rL}{V}$ .

Inviscid effects are represented in the generalized added inertia matrix [11], which can be simplified due to vehicle symmetry and effective terms.

$$\mathbf{M}_f = \begin{pmatrix} \mathbf{M}_f & \mathbf{C}_f^T \\ \mathbf{C}_f & \mathbf{J}_f \end{pmatrix} = - \begin{pmatrix} X_{\dot{u}} & 0 & 0 & 0 & 0 & 0 \\ 0 & Y_{\dot{v}} & 0 & 0 & 0 & Y_{\dot{r}} \\ 0 & 0 & Z_{\dot{w}} & 0 & Z_{\dot{q}} & 0 \\ 0 & 0 & 0 & K_{\dot{p}} & 0 & 0 \\ 0 & 0 & M_{\dot{w}} & 0 & M_{\dot{q}} & 0 \\ 0 & N_{\dot{v}} & 0 & 0 & 0 & N_{\dot{r}} \end{pmatrix} \quad (4)$$

Where  $\mathbf{M}_f$ ,  $\mathbf{C}_f$ , and  $\mathbf{J}_f$  represent the added mass, hydrodynamic coupling, and added inertia respectively. Additionally,  $Y_{\dot{r}} = N_{\dot{v}}$  and  $Z_{\dot{q}} = M_{\dot{w}}$ .

The terms in the added inertia matrix are calculated

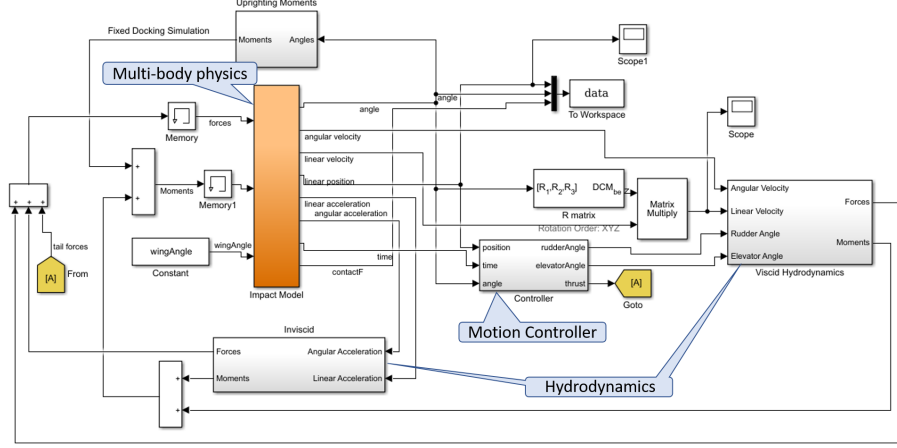


Fig. 4: The co-simulation architecture joins the hydrodynamic motion control model and multi-body physics model. The simulation was run to optimize the impact velocity with respect to capture envelope and peak impact force.

following

$$\begin{aligned} X'_u &= \frac{X_u}{0.5\rho L^3} & K'_p &= \frac{K_p}{0.5\rho L^5} \\ Y'_v &= \frac{Y_v}{0.5\rho L^3} & M'_q &= \frac{M_q}{0.5\rho L^5} \\ Z'_w &= \frac{Z_w}{0.5\rho L^3} & N'_r &= \frac{N_r}{0.5\rho L^5} \\ Y'_r = N'_v &= \frac{Y_r}{0.5\rho L^4} & Z'_q = M'_w &= \frac{Z_q}{0.5\rho L^4} \end{aligned} \quad (5)$$

Where the terms are non-dimensionalized using  $0.5\rho L^3$ ,  $0.5\rho L^4$ , and  $0.5\rho L^5$ . The resulting matrix can then be used to calculate resulting forces due to fluid inertia following Eqn. 6 [14].

$$\begin{bmatrix} \mathbf{f}_i \\ \mathbf{m}_i \end{bmatrix} = -\mathbf{M}_f \begin{bmatrix} \dot{\mathbf{v}}_1 \\ \dot{\mathbf{v}}_2 \end{bmatrix} \quad (6)$$

The impact between AUV and docking station is modelled following the approach in [9] using a force-indentation model, Eqn. 7 [15].

$$F = F_c(\delta) + F_v(\delta, \dot{\delta}) + F_p(\delta, \dot{\delta}) \quad (7)$$

In the force-indentation model,  $F_c$ ,  $F_v$ , and  $F_p$  are the elastic, viscous damping, and dissipative parts of the impact force and  $\delta$ ,  $\dot{\delta}$  are the penetration and penetration rate. Based on the key assumptions at the start of this section, no plastic deformation can be assumed simplifying the model to a spring-damper with  $k$  stiffness,  $e$  force exponent, and  $c$  damping coefficient. In the model, friction is approximated using a Coulomb approach.

$$F = k\delta^e + c\dot{\delta} \quad (8)$$

For the purposes of this work, we modelled the Dolphin II AUV [9], [16]. This AUV is 2.47m long, 0.2m diameter, and weighs 79.5kg. Simulation results presented here focus on

the optimization of impact velocity. If the impact velocity is too high the AUV tends to bounce along the docking station simplified funnel pieces. Conversely, if the impact velocity is too low the AUV can fail to dock as it lacks the thrust to effectively slide along the simplified funnel and ramp into the receiver. The optimization was completed when ramp angle was  $30^\circ$  and wing sweep angle was  $67.5^\circ$ . Optimization of the ramp and sweep angles are outside the scope of this work.

To optimize the AUV impact velocity, 20 different forward velocities were explored ranging from  $0.8m/s$  to  $3.0m/s$ . This velocity range covers the range of controllable docking velocities for the vehicle. For each of these velocities, a 70 point linearly spaced pattern was explored on the  $+Y$  side of the docking station. Due to symmetry of the docking station, results from  $+Y$  can be mirrored to  $-Y$ . The 70 point pattern imitates the effects of environmental disturbances.

Simulation of the docking system was completed in a hydrodynamic motion control and multi-body physics co-simulation environment. MATLAB was used to account for vehicle hydrodynamics and integrate the AUV's motion controller. ADAMS was used to account for the multi-body physics including impact force calculation and inertia. The co-simulation architecture is presented in Fig. 4.

The dynamic model is numerically solved in the ADAMS-/MATLAB co-simulation environment. The AUV is assumed to start 20 meters from the docking station. A traditional PD controller on both rudder and elevator is used to drive the AUV towards the desired target point for the first 18 meters of travel. When the AUV is 2 meters from the docking station, the controller switches to a PD controller that attempts to maintain a zero pitch, zero yaw state relative to the docking station. Each of the 1400 simulations recorded impact force, position, and angle of the AUV during its approach. The results were processed to determine size of successful capture area as well as maximum impact force.

#### IV. SIMULATION RESULTS

To determine optimal impact velocity with regards to capture envelope and maximum impact force, 1400 co-simulations were recorded and analyzed. Capture envelope was calculated by Eqn. 9.

$$\text{Capture Envelope} = 0.0025 \frac{m^2}{\text{trial}} \cdot n_{\text{success}} \quad (9)$$

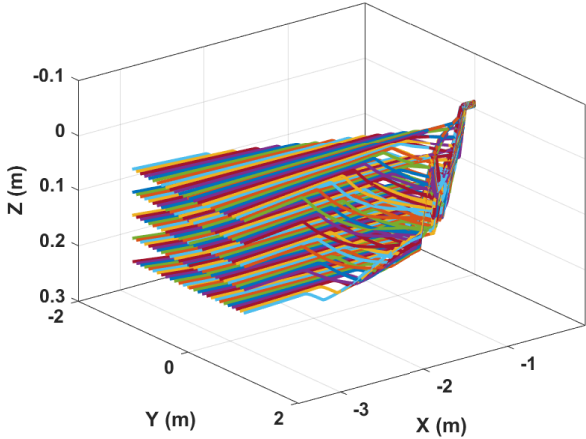


Fig. 5: Trajectories followed for docking at  $1.0\text{m/s}$ . The trajectories all end in the docking station located at  $(0, 0, 0)$

Number of successful trials ( $n_{\text{success}}$ ) was determined based on the final location of the AUV after completing the docking simulation. Docking was considered successful if the final location was inside of the area bounded by  $Y = \pm 0.2\text{m}$  and  $Z = \pm 0.1\text{m}$ . If the final AUV position is within these bounds its final location must be inside of the docking receiver so a bound on  $X$  proved to be unnecessary. The  $0.0025 \frac{m^2}{\text{trial}}$  constant is due to the 70 point scatter over a  $0.175\text{m}^2$  area and symmetry (effectively a 140 point scatter over  $0.35\text{m}^2$ ). Some of the trajectories completed are shown in Fig. 5. In this figure the AUV approaches the docking station located at  $(0, 0, 0)$  and bounces along the frame pieces into the receiver until docked.

Successful docking attempts were then clustered based on target impact velocity. Fig. 6 presents the effective capture area at each of the simulated impact velocities. From these results, a target impact velocity of between  $1.0\text{m/s}$  and  $2.0\text{m/s}$  is optimal. This relatively high impact velocity is partly due to the constant thrust assumption. With a constant thrust, at low velocities the thrust is not enough to overcome the friction involved in the docking maneuver thus slightly reducing the effective capture area. As impact velocity increases above  $2.0\text{m/s}$  the effective capture envelope quickly drops off. This drop off is due to the AUV bouncing along the guides rather than sliding into the station. The bouncing motion has a greater likelihood of jamming in the station or rolling the AUV. Between  $1.0\text{m/s}$  and  $2.0\text{m/s}$  the effective capture area is the full scale of the docking station at  $0.35\text{m}^2$ . This implies that in this velocity range as long as

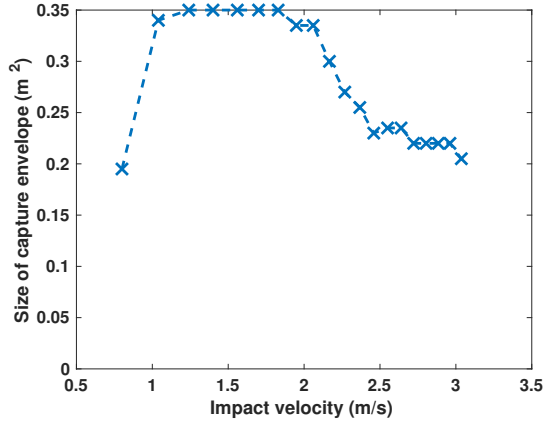


Fig. 6: The optimal impact velocity to maximize capture area is between  $1.0\text{m/s}$  and  $2.0\text{m/s}$ . As the velocity decreases below this range the vehicle loses control authority. As the velocity increases above the optimal range, the AUV enters a bouncing mode of motion resulting in less capture area.

the docking adapter contacts the docking station the AUV will successfully dock.

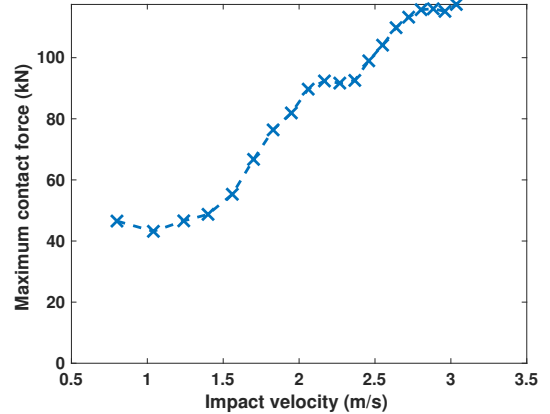


Fig. 7: The optimal impact velocity to minimize impact force is  $1.0\text{m/s}$  in simulation. Maximum impact force at this velocity is  $43\text{kN}$ .

Maximum impact force experienced during either successful or failed docking attempts defines the strength required for the design. To adequately support docking, the design must be able to support the worst case impact without sustaining any permanent damage. Fig. 7 shows the maximum contact force for the tested velocities. As expected, when the impact velocity is high (above  $2.0\text{m/s}$ ), the impact force grows quite quickly up to  $120\text{kN}$ . At low velocities the maximum impact force decreases to  $43\text{kN}$  at  $1.0\text{m/s}$ . The initial assumption for maximum impact force was that it would decrease linearly with impact velocity as the initial impact force would be directly related to the impact velocity. The maximum impact force however does not always occur on the first impact. In some cases the second contact between AUV and docking station is the peak impact force as the

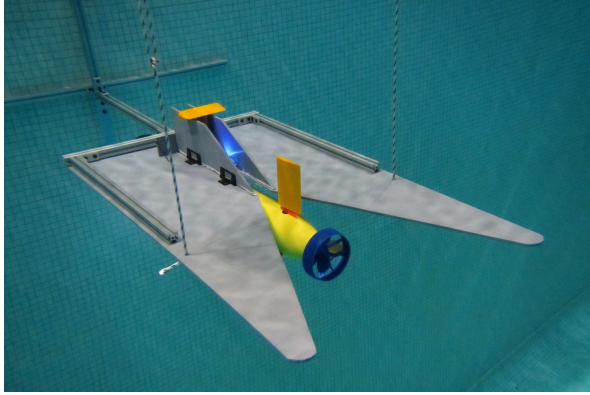


Fig. 8: Prototype dock and SandShark during pool testing.

AUV has bounced from one guide piece with a small angle of reflection to another one with a larger angle. This non-linearity causes the minimum impact force to be at  $1.0m/s$  in the simulation. Although a more exhaustive optimization would likely smooth out this nonlinear maximum force, for the purposes of this paper we do not expect it would change the results significantly.

Based on this analysis with the Dolphin II AUV, the terminal homing stage of docking should be completed at  $1.0m/s$ . This velocity gives the AUV ample control authority, enough time for sensor correction, and leads to the optimal capture scenario. With an optimal impact velocity of  $1.0m/s$ , the maximum impact force that can be expected is  $43kN$  and the capture area is the full scale of the docking station at  $0.35m^2$ .

## V. CONCLUSIONS & FUTURE WORK

The new docking station presented in this paper intends to extend AUV operational period indefinitely through the use of underwater recharging. The station has many key features that make it a good candidate for widespread adoption: 1) it is able to support a wide range of AUVs with minimal modification of the AUV required. 2) it has a large capture envelope relative to body size meaning that it can be deployed at reduced cost. 3) it can easily be scaled to support multiple AUVs through the use of charging trees.

This paper presented the optimization of the impact velocity during terminal homing and capture using a constant thrust assumption. Based on the results, an impact velocity of  $1.0m/s$  is ideal to minimize maximum contact force and maximize capture envelope for the Dolphin II AUV. When impacting at this velocity, the peak impact force is  $43kN$  and the capture envelope is  $0.35m^2$ , or the entire feasible capture area. Different scale AUVs may have faster, or slower optimal docking speeds.

Future work with the docking station will be to begin prototyping of the docking station and experimental validation,

Fig. 8. This will initially be completed in a controlled environment using both a Bluefin SandShark and an OceanServer Iver 3. Following initial validation, the docking station will be taken outside to confirm performance in open water. Docking trees will be validated as will the deployment and recovery process. One of the primary motivations behind the unique design is to create a mobile docking station. Following further optimization of the hydrodynamic performance of the station it will be put onto an AUV to enable AUV-AUV docking and power transfer.

## REFERENCES

- [1] T. B. Curtin, J. G. Bellingham, J. Catipovic, and D. Webb, “Autonomous oceanographic sampling networks,” *Oceanography*, vol. 6, no. 3, pp. 86–94, 1993. [Online]. Available: <http://www.jstor.org/stable/43924649>
- [2] J. G. Bellingham, *Autonomous Underwater Vehicle Docking*. Cham: Springer International Publishing, 2016, pp. 387–406. [Online]. Available: [https://doi.org/10.1007/978-3-319-16649-0\\_16](https://doi.org/10.1007/978-3-319-16649-0_16)
- [3] T. Podder, M. Sibenac, and J. Bellingham, “Auv docking system for sustainable science missions,” in *Robotics and Automation, 2004. Proceedings. ICRA '04. 2004 IEEE International Conference on*, vol. 5, April 2004, pp. 4478–4484 Vol.5.
- [4] R. S. McEwen, B. W. Hobson, L. McBride, and J. G. Bellingham, “Docking control system for a 54-cm-diameter (21-in) auv,” *IEEE Journal of Oceanic Engineering*, vol. 33, no. 4, pp. 550–562, Oct 2008.
- [5] R. Stokey, B. Allen, T. Austin, R. Goldsborough, N. Forrester, M. Purcell, and C. von Alt, “Enabling technologies for remus docking: an integral component of an autonomous ocean-sampling network,” *IEEE Journal of Oceanic Engineering*, vol. 26, no. 4, pp. 487–497, Oct 2001.
- [6] H. Singh, J. G. Bellingham, F. Hover, S. Lemer, B. A. Moran, K. von der Heydt, and D. Yoerger, “Docking for an autonomous ocean sampling network,” *IEEE Journal of Oceanic Engineering*, vol. 26, no. 4, pp. 498–514, Oct 2001.
- [7] A. Sans-Muntadas, K. Y. Pettersen, E. Brekke, and V. F. Henriksen, “A hybrid approach to underwater docking of auvs with cross-current,” in *OCEANS 2016 MTS/IEEE Monterey*, Sept 2016, pp. 1–7.
- [8] K. Teo, E. An, and P. P. J. Beaujean, “A robust fuzzy autonomous underwater vehicle (auv) docking approach for unknown current disturbances,” *IEEE Journal of Oceanic Engineering*, vol. 37, no. 2, pp. 143–155, April 2012.
- [9] T. Zhang, D. Li, and C. Yang, “Study on impact process of AUV underwater docking with a cone-shaped dock,” *Ocean Engineering*, vol. 130, pp. 176 – 187, 2017. [Online]. Available: <http://www.sciencedirect.com/science/article/pii/S0029801816305807>
- [10] S. Peng, C. Yang, S. Fan, S. Zhang, P. Wang, and Y. Chen, “Hybrid underwater glider for underwater docking: modeling and performance evaluation,” *Marine Technology Society Journal*, vol. 48, no. 6, pp. 112–124, 2014.
- [11] T. I. Fossen, *Guidance and control of ocean vehicles*. John Wiley & Sons Inc, 1994.
- [12] R. C. Nelson, *Flight stability and automatic control*. WCB/McGraw Hill New York, 1998, vol. 2.
- [13] B. N. Pamadi, *Performance, stability, dynamics, and control of airplanes*. AIAA, 2004.
- [14] C. Brennen, “A review of added mass and fluid inertial forces.” BRENNEN (CE) SIERRA MADRE CA, Tech. Rep., 1982.
- [15] S. Faik and H. Witteman, “Modeling of impact dynamics: A literature survey,” in *2000 International ADAMS User Conference*, vol. 80, 2000.
- [16] M. Zhang, Y. Xu, B. Li, D. Wang, and W. Xu, “A modular autonomous underwater vehicle for environmental sampling: System design and preliminary experimental results,” in *OCEANS 2014 - TAIPEI*, April 2014, pp. 1–5.